Prediction of ambient superconductivity in ternary thorium-silicon superhydrides with a breathing kagome lattice

Xiaomeng Wang,[1,2] Chi Ding,[2] Qing Lu,[2] Tianheng Huang,[2] Yuhang Li,[1] Junjie Wang,[2,*] Yu Han,[2] Dingyu Xing,[2] and Jian Sun[2,†]

[1]*School of Physics, Ningxia University, Yinchuan 750021, People's Republic of China*

[2]*National Laboratory of Solid State Microstructures, School of Physics and Collaborative Innovation Center of Advanced Microstructures, Nanjing University, Nanjing 210093, People's Republic of China*

(Received 20 September 2023; revised 5 June 2024; accepted 1 July 2024; published 23 July 2024)

A major focus of current research on superconducting superhydrides is to achieve superconductivity at lower pressures, especially ambient pressure. Here we present the prediction of a class of high-temperature ternary hydrogen-rich superconductors, which are metastable at mild pressure and dynamically stable at ambient pressure using crystal structure searching. Our findings reveal the existence of a hexagonal $ThSiH_7$ compound with a superconducting T_c of 61.5 K at ambient pressure, as estimated by electron-phonon coupling calculations. Interestingly, the H sites in $ThSiH_7$ materialize a breathing kagome network, equivalent to a triangular lattice of trimer plaquettes, which is entirely different from previously known hydrogen clathrate structures. By substituting Th with lanthanide elements, we discovered that $LaSiH_7$ and $CeSiH_7$ are also dynamically stable at 0 GPa, while $PrSiH_7$ and $NdSiH_7$ are dynamically stable at 10 and 15 GPa with high T_c values of 63.9 and 65.9 K, respectively. Our results provide a system for superconducting hydrides and open a promising avenue for studying ambient pressure high-temperature superconductors.

DOI: 10.1103/PhysRevB.110.024513

I. INTRODUCTION

Metallic hydrogen has long held the promise of exhibiting superconductivity near or even above room temperature at ultrahigh pressure; however, the required experimental conditions are extremely strict [1]. Subsequently, Ashcroft proposed a concept involving "chemical precompression" by utilizing the influence of other elements to achieve superconducting hydrides at lower pressure conditions [2]. Following this proposal, both theoretical and experimental breakthroughs have been made in the study of binary hydrogen-rich, high-temperature superconductors under high pressure, triggering the "hydride rush" and breaking the successive records of superconducting transition temperatures [3–7]. In recent years, inspired by theoretical predictions, many hydrogen-rich binary compounds have been successfully synthesized [8–14].

While the prospect of room-temperature superconductivity is undoubtedly appealing, the attainment of this state in hydrogen-rich compounds typically necessitates extremely high pressures, thereby limiting their practical applications. Consequently, recent research endeavors have shifted towards reducing the stable pressure conditions required for hydrogen-based superconductors. One idea is to use doping or substitution with different elements and investigate the phase diagrams of ternary or quaternary hydrides, which provides a vast and rich phase space of stable or metastable structural prototypes for superconducting superhydride screening [15,16]. For example, Zhang *et al.* [17] identified a "fluorite-type" backbone in compositions of the form AXH_8, which exhibit high-temperature superconductivity at moderate pressures compared with other reported hydrogen-based superconductors. Moreover, recent experimental works have reported giant enhancement of superconducting properties in the La-Ce-H system [18–20]. In addition, a careful choice of the suitable doping elements also plays a crucial role. For example, partially replacing 3% of the Ca atoms in $Ca(BH_4)_2$ with K atoms results in an estimated T_c of 110 K at ambient pressure [21].

In most of the rare-earth (RE) hydride systems studied, substantially H-richer REH_9 species exhibiting peculiar three-dimensional H clathrate structures of H_{29} cages were identified [22–28]. Among these, ThH_9 has the highest T_c of 146 K [22]. The clathrate structures provide a feasible way to use suitably selected atoms as doping to construct ternary alloy superhydrides that share the same crystal structure. In addition, considering that Th_4H_{15} is the first reported superconductor with a relatively high T_c of 8 K at ambient pressure among the metal hydrides [29], it is highly interesting to introduce dopant elements into the parent ThH_9 system to establish a ternary platform for realizing a superconductor that works at both high temperatures and relatively low pressure.

In this paper, we report a theoretical prediction of superconductivity at ~62 K and ambient pressure in a metastable structure of $ThSiH_7$ with $P\bar{6}m2$ phase, setting a new record among ambient superconductivity in hydrides. This structure has extended our searches into other RE element hydrides, from which we found five dynamically stable H-based

*Contact author: wangjunjie@nju.edu.cn
†Contact author: jiansun@nju.edu.cn

superconductors below 20 GPa, consisting of RE element X (X = La, Ce, Pr, Nd, Sm). An analysis of electronic and superconducting properties indicates prominent influence of the electron donation and chemical pressure of the Th and Si atoms on the significantly enhanced T_c and pressure stability into the ambient regime in $ThSiH_7$.

II. RESULTS AND DISCUSSION

Using the idea of a "precompressed" hydrogen-based alloy backbone, we designed a H-Si alloy backbone by substituting the H atoms which sit on the 2*a* (0,0,0.5) Wyckoff position in the $P6_3/mmc$ ThH_9 [22] with the Si atom, resulting in a unique ternary alloy superhydride $P6_3/mmc$ $ThSiH_7$ as the model system (Fig. S1 of the Supplemental Material [30]). This structure achieves the precompression mechanism very efficiently: in addition to the Th atoms, the Si atoms at the center of the triangular-prism H_6 units, also exert an additional pressure on the hydrogen sublattice, lowering the minimum stable pressure. Phonon calculation indicates that $P6_3/mmc$ $ThSiH_7$ is dynamically stable at 0 GPa, exhibiting no imaginary phonon modes (Fig. S2).

The above attempt indicates that the Th-Si-H system is promising in finding ambient pressure stable superhydrides. With this idea in mind, we used our own-developed MAGUS code (machine learning and graph theory assisted universal structure searcher) to explore the crystal structures in the ternary Th-Si-H system below 50 GPa, focusing on H-rich species [31,32]. Density functional theory calculations were performed with the VASP code [33], accompanied with the projector augmented-wave method [34]. The electron-phonon couplings and superconductivity calculations were performed with density functional perturbation theory, as implemented in the QUANTUM ESPRESSO code [35].

Our structure predictions show three hydrogen-rich compounds: $ThSiH_{10}$, $ThSiH_7$, and $ThSiH_2$. Among these structures, we focus on $ThSiH_7$, which has the same composition as $P6_3/mmc$ constructed manually above. The most stable phase obtained for $ThSiH_7$ has $P3$ symmetry. We also found a metastable phase in $ThSiH_7$ with $P\bar{6}m2$ symmetry. As shown in Fig. 1(a), we have systematically calculated the enthalpy as a function of pressure for Th-Si-H structures relative to the phases of $ThSiH_7$ [46–52], and found that $P3$ $ThSiH_7$ becomes thermodynamically stable above 11.0 GPa. However, we are more interested in the $P\bar{6}m2$ structure. On the one hand, the $P\bar{6}m2$ phase can dynamically maintain stability under ambient pressure while the $P3$ phase is unstable. On the other hand, the H sites in $P\bar{6}m2$ $ThSiH_7$ materialize a breathing kagome network, which is entirely different from previously known hydrogen clathrate structures. Meanwhile, although the enthalpy of the $P\bar{6}m2$ structure is about 25.4 meV/atom higher than that of the $P3$ phase, the formation enthalpy of the $P\bar{6}m2$ structure at atmospheric pressure is still exothermic ($\Delta H = -351$ meV per formula unit), indicating that the structure is at least thermodynamically metastable. Materials can become trapped in local energy minima, known as metastable states, within the energy landscape during the process of experimental synthesis. Therefore, metastable materials are actually not rare and widely studied [53–56]. In fact, 20% of the materials in the Inorganic Crystal Structure Database are metastable. Therefore, the $P\bar{6}m2$ phase of $ThSiH_7$ may also appear in future experiments.

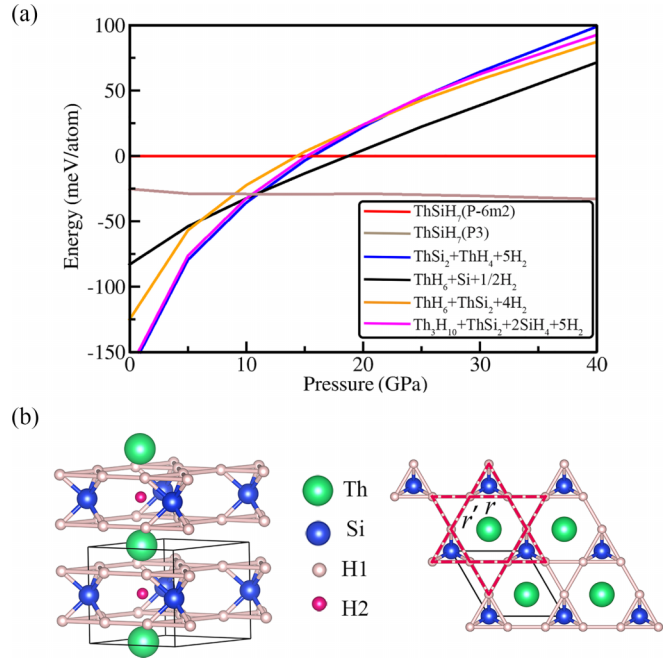

FIG. 1. Energetic stability of the Th-Si-H system under pressure and the crystal structure of a H-based breathing kagome lattice. (a) Calculated enthalpy as a function of pressure for Th-Si-H structures relative to the $P\bar{6}m2$ phase of $ThSiH_7$. (b) Hexagonal unit cell of $ThSiH_7$; within the SiH_6 layer, H atoms form a distorted kagome net, with alternating distances r, r' between nearest neighbors. The green, blue, and pink spheres represent Th, Si, and H atoms, respectively.

For illustrative purposes, the $P\bar{6}m2$ structure may be decomposed into SiH_7 layers and perfectly planar Th sheets stacked along the c axis, as shown in Fig. 1(b). The H1 sites sit at the vertices of a triangular prism centered around Si atoms, materialize a breathing kagome network, equivalent to an alternate arrangement of two different equilateral triangles with corner sharing. There is another H2 site, sitting in the center of the cage formed by two [H_6] rings and three Si atoms. A quantitative measure of the distortion away from the ideal kagome structure is the ratio between alternating (breathing) nearest (r) and next-nearest (r') neighbor H-H distances. Supplemental Fig. S6 shows the calculated lattice parameter, Si-H bond length, and H-H bond lengths within the breathing kagome network as a function of pressure up to 40 GPa. The nearest (r) neighbor H-H distance exhibits an obvious variation under pressure, while the next-nearest (r') neighbor H-H distance and the Si-H bond length are almost unchanged, resulting in $r/r' = 0.99$ at 0 GPa and $r/r' = 0.82$ at 40 GPa. This implies compression has little effect on the interaction between Si and H atoms, and we believe that the strong interactions between Si and H atoms play an important role in determining its relatively low-pressure dynamical stability.

A great deal of previous work has shown that the substitution of elements within carefully chosen host crystals plays an important role in enhancing T_c. Given that RE metals have similar electronic configurations, atomic radii, and small

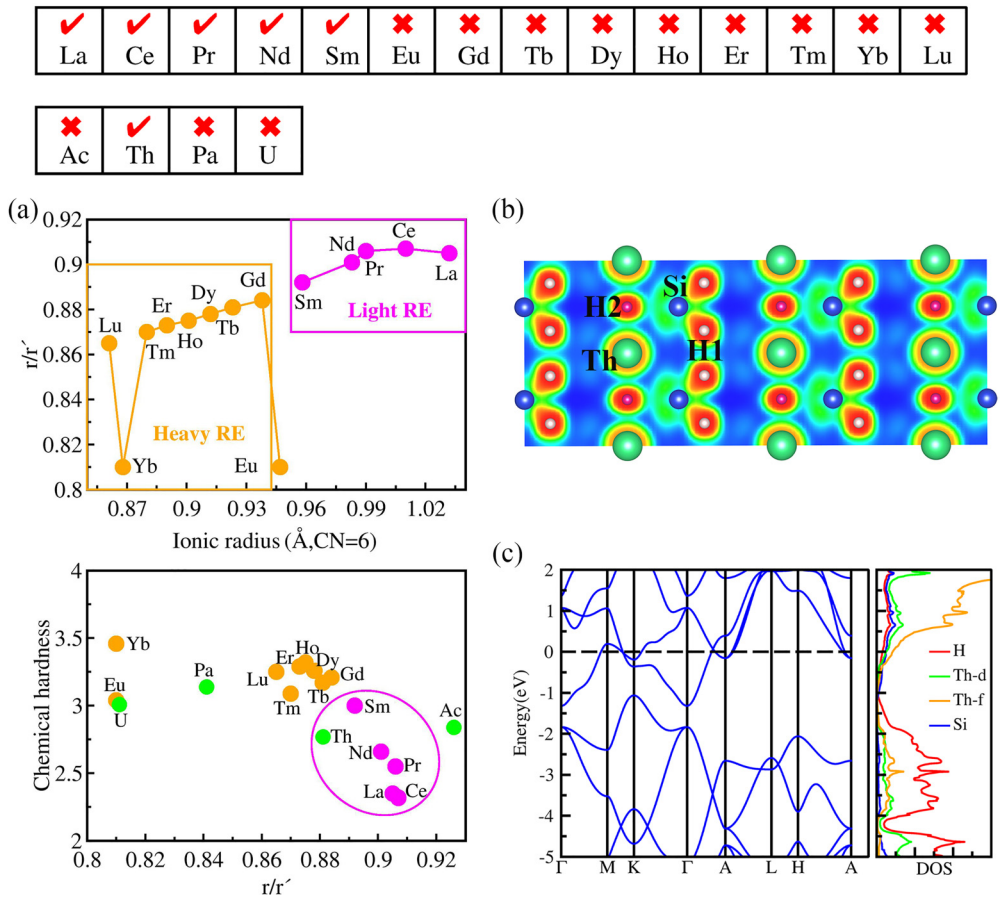

FIG. 2. Elemental composition and electronic properties of $P\bar{6}m2$ $ThSiH_7$ at 0 GPa. (a) Dynamical stability of the $RESiH_7$ structure at 20 GPa for substitution with other RE elements. Dynamically stable and unstable compounds are indicated by ticks and crosses, respectively. A general trend of decreasing the ratio between alternating nearest (r) and next-nearest (r') neighbor H-H distances with the reduction of the ionic radius of RE^{3+}. The ratio r/r' and chemical hardness can be rationally correlated with the dynamic stability as evident clustering is observed. (b) The calculated ELF with isosurface value of 0.8 and ELF in the (110) plane. (c) The band structures and partial density of states of $P\bar{6}m2$ $ThSiH_7$ at 0 GPa.

electronegativities in the range of 1.0–1.36 on the Pauli scale, it is expected to achieve comparable high temperature and relatively low pressure in other $RESiH_7$ with the same crystal structure by replacing Th with other RE elements. Aiming at identifying compounds with low critical pressures, we performed structural relaxations at 20 GPa for all combinations of RE = [all of lanthanides, Ac, Pa, and U] in the $P\bar{6}m2$ phase of the $RESiH_7$ template, and evaluated the dynamical stability of the resulting compounds by calculating the phonon dispersions. Among the resulting 17 combinations investigated, only five lanthanide series compounds exhibit dynamic stability within the pressure range of 20 GPa [Fig. 2(a)]. Notably, $LaSiH_7$ and $CeSiH_7$ remain dynamically stable even at ambient pressure.

To discuss the physical reasons behind the dynamic stability of these hydrides, we have to consider the differences in the physical and chemical properties of these RE elements. The most important properties, such as electronegativities, the ionic radius of RE^{3+}, ionization energy, chemical hardness, and electronic configurations, for the 18 RE elements at ambient pressure are shown in Supplemental Material Table SII. Here, for convenience, we label compounds that are stable below 20 GPa as $XSiH_7$ (X including lanthanide elements La, Ce, Pr, Nd, Sm and actinide element Th). As shown in Fig. 2(a), we find that the ionic radius of RE^{3+} can be rationally correlated with the r/r', as there is an evident general trend of decreasing r/r' with the reduction of the ionic radius observed. Further, it is expected that the chemical hardness, which quantifies the stability of the neutral state of the atom, can play an important role in determining the stability of the $XSiH_7$. Parr and Pearson defined the chemical hardness as [57]

$$\eta = \frac{1}{2}\left(\frac{\partial^2 E}{\partial N^2}\right)_Z \approx (E_i - E_a)/2,$$

where E, N, E_i, E_a, and Z are the total energy, number of electrons, ionization energy, electron affinity, and atomic number of the chemical species, respectively. Finally, we utilize r/r' and chemical hardness [58] to associate with the dynamic stability of all systems including elements Ac, Pa, and U. As expected, we find that r/r' and chemical hardness can be reasonably correlated with stability, and we observe distinct clustering. Previous work has indicated that the small values for the increase in chemical hardness with covalent bonding and low chemical hardness facilitates the formation of multicenter covalent bonding, and metallic bonding itself can be

regarded as the extreme case of multicenter covalent bonding [59]. It is worth noting that the chemical hardness of Si is lower than that of other nonmetallic elements. An increase in the chemical hardness of the [SiH_6] group can be anticipated, but due to the covalent nature of the bonding, the magnitude of the increase is relatively small. Meanwhile, we found that the chemical hardness for candidate elements X is lower than 2.8 eV. This means that relatively low-pressure dynamical stability in $X SiH_7$ systems correlates strongly with strong X-H and Si-H bonding.

We examine the chemical bonding of the $X SiH_7$ structures by analyzing the electron localization function (ELF), Bader charge transfer, and the crystal orbital bond index (COBI) [42]. As shown in Fig. 2(b) and Supplemental Figs. S9–S13, the ELF slice of the (110) plane containing X = [Th, La, Ce, Pr, Nd, Sm], Si, and H atoms shows that (i) there is no charge localization between the X and H atoms, indicative of an ionic character between X and H; and (ii) the ELF values between the Si and H atoms gradually increase toward the H atoms, indicating the polar covalent character of the Si-H bonds. Bader charge analysis reveals a large amount of charge transfer to the H atoms from nearby Si and X atoms (Table SIII of the Supplemental Material). Take $ThSiH_7$ as an example: each Th atom and Si atom loses 2.03 and 2.00 electrons, respectively. Correspondingly, each H atom (H1) in [SiH_6] units accept 0.59 electrons and the isolated H atom (H2) gets 0.50 electrons. As shown in Fig. S8, the energy-integrated values (up to the Fermi level) of crystal orbital bond index, namely ICOBI, for the Si-H, Th-H, and H-H bonds equals 0.41, 0.31, and 0.02, respectively, indicating a strongly covalent contribution of Si-H and Th-H, which fulfill the expectation. Furthermore, using minus projected crystal orbital hamilton populations (−pCOHP), we can partition the bond energy into bonding states with positive values and antibonding states with negative values. As shown in Fig. S14, these electrons occupy antibonding orbitals along the H-H bonds, resulting in longer H-H distances ($d_{H-H} \sim 2.2A$) and the weakening of the H-H bonding, as well as giving rise to an increased H-projected density of states (H-PDOS) at the Fermi level. With increasing pressure, the number of electrons transferred by Th and Si atoms decreases and increases, respectively. The results indicate that the Si-H bonds in $ThSiH_7$ are much stronger than H-H interactions in cage hydrogen-rich compounds, and the Si and H atoms can maintain a strong bonding interaction over large pressure range.

Our main concern is whether these hydrides still have the superconducting properties at ambient pressure. In Fig. 2(c) and Supplemental Figs. S9–S13, we first show the electronic structure, along with the partial density of states for these hydrides. Band structure analysis reveals that except for $SmSiH_7$, all of them are metallic phases with a large total electronic density of states and the bands around the Fermi level derive from the hybridization with the H, Si, and X atoms. Consequently, the hydrogen-rich $X SiH_7$ compounds have the potential to demonstrate favorable superconducting characteristics.

To examine the potential superconductivity in these structures, in Fig. 3(a) and Supplemental Figs. S9–S12, the phonon dispersions decorated with the partial electron-phonon (e-ph) coupling coefficients λ, together with the atom-projected Eliashberg function $\alpha^2F(\omega)$ and the phonon density of states were performed with density functional perturbation theory. The projected phonon density of states of these hydrides can be separated into three regions. The X atom with the heaviest atomic mass dominates the low-frequency region (below 100 cm^{-1}), whereas the vibrations of the Si and H atoms are associated with the midfrequency (between 100 and 350 cm^{-1}) and high-frequency (above 350 cm^{-1}) phonon branches, respectively. For $ThSiH_7$, our e-ph calculation yields a λ of 1.47 at 0 GPa. The three modes with maximal coupling, depicted in Fig. 3(b), are (I) and (II), where the vibrations of the H atoms are in the *ab* plane, while the H2 vibrations are much stronger than those of the H1 atoms, and (III), where the H1-H1 stretching mode contains unique vibration directions. Note that in all three modes H atoms are involved. The modes of atomic H contribute 53% of the total λ, and the Si and Th atoms contribute 35% and 12%, respectively. The soft mode near 250 cm^{-1} at the Γ point makes an important contribution to the e-ph coupling. We adopted the Allen-Dynes modified McMillan equation to estimate the T_c of $ThSiH_7$ using the calculated logarithmic average ω_{log} and typical Coulomb pseudopotential parameters $\mu* = 0.1$, leading to a T_c of ∼61.5 K at 0 GPa. Likewise, as shown in Fig. 3(c), we investigated potential superconductivity in other structures and predicted that the T_c values for $LaSiH_7$ and $CeSiH_7$ are much lower at 41.2 and 20.7 K at 0 GPa, although for $PrSiH_7$ and $NdSiH_7$ as high as 63.9 K at 10 GPa and 65.9 K at 15 GPa due to the introduction of pressure, which enhances superconductivity.

Anharmonicity was found to play an important role in some superconducting hydrides [60,61]. Therefore, we present a first-principles analysis of the full anharmonic phonon spectra of $P\bar{6}m2$ $ThSiH_7$ at 0 GPa based on the variational stochastic self-consistent harmonic approximation method [62]. As illustrated in Fig. S15, the inclusion of anharmonic corrections induces significant alterations in the harmonic spectrum, particularly affecting the low-energy optical modes. Specifically, a significant softening occurs at the G and A points of the Brillouin zone due to anharmonicity, but the calculated T_c is slightly suppressed by anharmonicity. As shown in Fig. 4, a wide range of stable pressure and superconducting temperature values for superconducting hydrides can be seen [63]. The identification of $ThSiH_7$, as the intrinsically dynamically stable superconducting superhydride under ambient pressure, has the potential to significantly influence the field of materials science.

III. CONCLUSION

In summary, the focus in the search for hydrogen-based superconductors has evolved from solely aiming for high-temperature superconductivity to achieving a balance of low-pressure stability. Here, using our MAGUS method and first-principles calculations, we identified a ternary metastable hydride $P\bar{6}m2$ $ThSiH_7$ with a breathing kagome lattice of H atoms. Most importantly, compared to other reported H-based superconductors, our predicted $P\bar{6}m2$ $ThSiH_7$ exhibits dynamic stability at ambient pressure while maintaining a considerably high superconducting transition temperature (∼61.5 K). In addition, we also extended our investigations

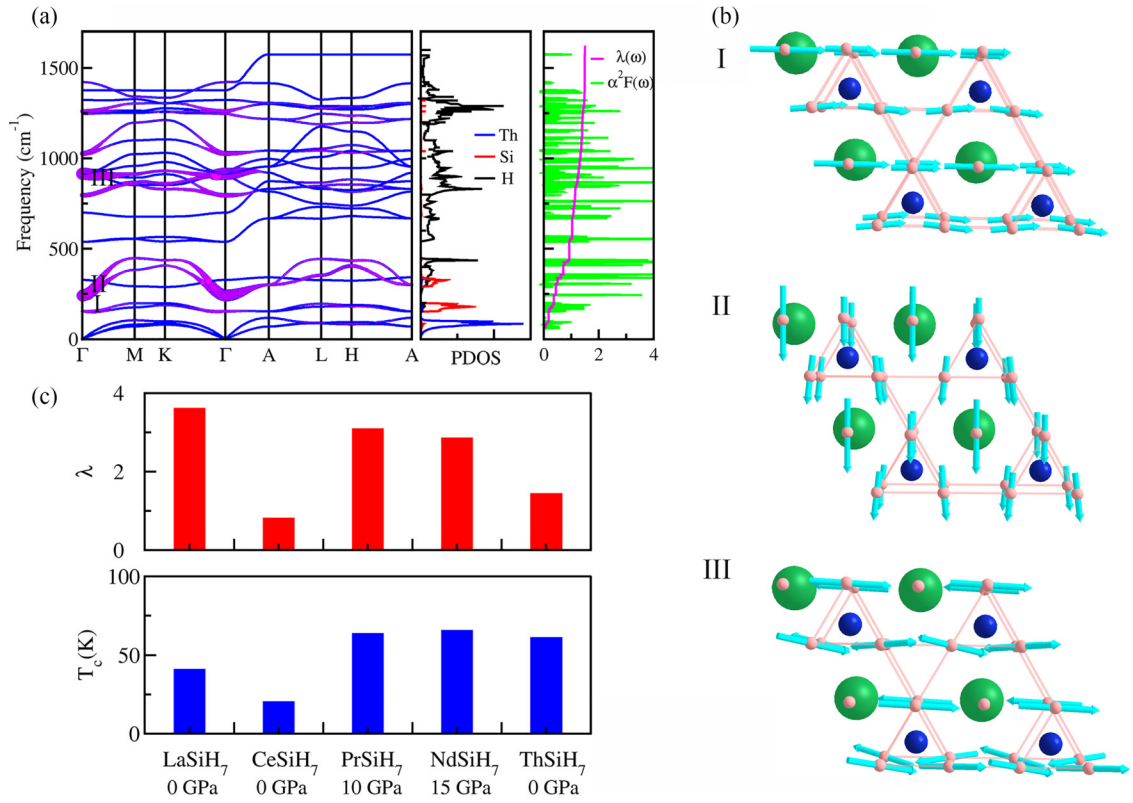

FIG. 3. Superconducting properties of $X\mathrm{SiH_7}$. (a) Phonon band structures, projected density of states, Eliashberg spectral function, and the electron-phonon coupling constant λ of $\mathrm{ThSiH_7}$ at 0 GPa. The sizes of these violet solid circles are proportional to the electron-phonon coupling strength. (b) Phonon modes with the strongest e-ph coupling, labeled as indicated in (a). (c) The calculated EPC parameter λ (top panel) and T_c (bottom panel) of $X\mathrm{SiH_7}$.

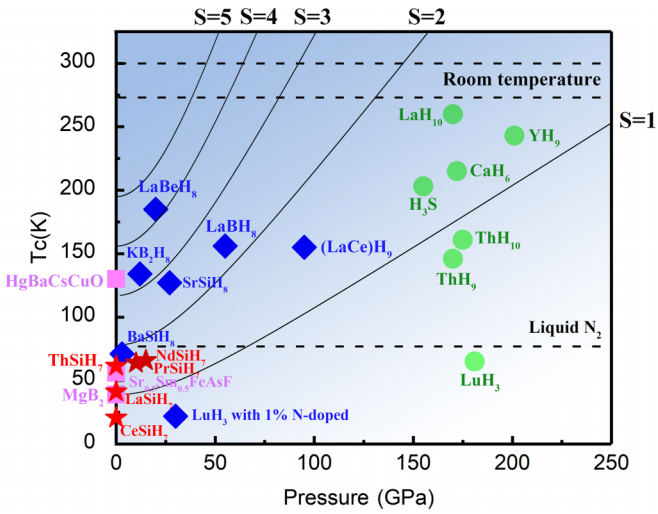

FIG. 4. Superconducting critical temperature, T_c, as a function of the pressure at which it has been calculated or measured for different hydrides. The purple stars correspond to predictions of this work. The blue rhombi are T'_cs of ternary hydrides at the lowest pressure where they become dynamically stable. Green circles are T'_cs of binary hydrides to experimental measurements. The pink squares are T'_cs of well-known superconductors from experiment at ambient pressure. The colored contours correspond to the figure of merit S proposed in equation $S = (T_c/\sqrt{T^2_{c,\,\mathrm{MgB_2}} + P^2})$.

to explore analogous structures derived from other RE elements (RE = all of lanthanides, Ac, Pa, and U) based on the $P\bar{6}m2$ $\mathrm{ThSiH_7}$ framework. Intriguingly, our findings indicate that certain derivatives within this series are also dynamically stable at ambient pressure. Our results demonstrate that constructing multiple element configurations is feasible in reducing the stable pressure of superhydrides while maintaining high-temperature superconductivity, and will usher in more discoveries in the search for the best inclusion complex superhydrides.

ACKNOWLEDGMENTS

We gratefully acknowledge financial support from the National Key R&D Program of China (Grant No. 2022YFA1403201), the National Natural Science Foundation of China (Grants No. 12304022, No. 12125404, and No. 52361035), the Basic Research Program of Jiangsu, and the Fundamental Research Funds for the Central Universities. J.W. is partially supported by the Postdoctoral Fellowship Program of CPSF under Grant No. GZC20240695. C.D. and J.W. are partially supported by the Jiangsu Funding Program for Excellent Postdoctoral Talent (Nos. 2024ZB002 and 2024ZB075). The calculations were carried out using supercomputers at the High Performance Computing Center of Collaborative Innovation Center of Advanced Microstructures, the high-performance supercomputing center of Nanjing University.

[1] N. W. Ashcroft, Metallic hydrogen: A high-temperature superconductor? Phys. Rev. Lett. **21**, 1748 (1968).

[2] N. W. Ashcroft, Hydrogen dominant metallic alloys: High temperature superconductors?, Phys. Rev. Lett. **92**, 187002 (2004).

[3] D. Duan, Y. Liu, F. Tian, D. Li, X. Huang, Z. Zhao, H. Yu, B. Liu, W. Tian, and T. Cui, Pressure-induced metallization of dense $(H_2S)_2H_2$ with high-T_c superconductivity, Sci. Rep. **4**, 6968 (2014).

[4] Y. Li, J. Hao, H. Liu, Y. Li, and Y. Ma, The metallization and superconductivity of dense hydrogen sulfide, J. Chem. Phys. **140**, 174712 (2014).

[5] H. Liu, I. I. Naumov, R. Hoffmann, N. W. Ashcroft, and R. J. Hemley, Potential high-T_c superconducting lanthanum and yttrium hydrides at high pressure, Proc. Natl. Acad. Sci. USA **114**, 6990 (2017).

[6] F. Peng, Y. Sun, C. J. Pickard, R. J. Needs, Q. Wu, and Y. Ma, Hydrogen clathrate structures in rare earth hydrides at high pressures: Possible route to room-temperature superconductivity, Phys. Rev. Lett. **119**, 107001 (2017).

[7] H. Wang, J. S. Tse, K. Tanaka, T. Iitaka, and Y. Ma, Superconductive sodalite-like clathrate calcium hydride at high pressures, Proc. Natl. Acad. Sci. USA **109**, 6463 (2012).

[8] A. P. Drozdov, M. I. Eremets, I. A. Troyan, V. Ksenofontov, and S. I. Shylin, Conventional superconductivity at 203 kelvin at high pressures in the sulfur hydride system, Nature (London) **525**, 73 (2015).

[9] A. P. Drozdov, P. P. Kong, V. S. Minkov, S. P. Besedin, M. A. Kuzovnikov, S. Mozaffari, L. Balicas, F. F. Balakirev, D. E. Graf, V. B. Prakapenka *et al.*, Superconductivity at 250 K in lanthanum hydride under high pressures, Nature (London) **569**, 528 (2019).

[10] M. Somayazulu, M. Ahart, A. K. Mishra, Z. M. Geballe, M. Baldini, Y. Meng, V. V. Struzhkin, and R. J. Hemley, Evidence for superconductivity above 260 K in lanthanum superhydride at megabar pressures, Phys. Rev. Lett. **122**, 027001 (2019).

[11] P. Kong, V. S. Minkov, M. A. Kuzovnikov, A. P. Drozdov, S. P. Besedin, S. Mozaffari, L. Balicas, F. F. Balakirev, V. B. Prakapenka, S. Chariton *et al.*, Superconductivity up to 243 K in the yttrium-hydrogen system under high pressure, Nat. Commun. **12**, 5075 (2021).

[12] E. Snider, N. Dasenbrock-Gammon, R. McBride, X. Wang, N. Meyers, K. V. Lawler, E. Zurek, A. Salamat, and R. P. Dias, Synthesis of yttrium superhydride superconductor with a transition temperature up to 262 K by catalytic hydrogenation at high pressures, Phys. Rev. Lett. **126**, 117003 (2021).

[13] L. Ma, K. Wang, Y. Xie, X. Yang, Y. Wang, M. Zhou, H. Liu, X. Yu, Y. Zhao, H. Wang *et al.*, High-temperature superconducting phase in clathrate calcium hydride CaH_6 up to 215 K at a pressure of 172 GPa, Phys. Rev. Lett. **128**, 167001 (2022).

[14] Z. Li, X. He, C. Zhang, X. Wang, S. Zhang, Y. Jia, S. Feng, K. Lu, J. Zhao, J. Zhang *et al.*, Superconductivity above 200 K discovered in superhydrides of calcium, Nat. Commun. **13**, 2863 (2022).

[15] K. P. Hilleke and E. Zurek, Tuning chemical precompression: Theoretical design and crystal chemistry of novel hydrides in the quest for warm and light superconductivity at ambient pressures, J. Appl. Phys. **131**, 070901 (2022).

[16] X. Zhang, Y. Zhao, and G. Yang, Superconducting ternary hydrides under high pressure, WIREs Comput. Mol. Sci. **12**, e1582 (2022).

[17] Z. Zhang, T. Cui, M. J. Hutcheon, A. M. Shipley, H. Song, M. Du, V. Z. Kresin, D. Duan, C. J. Pickard, and Y. Yao, Design principles for high-temperature superconductors with a hydrogen-based alloy backbone at moderate pressure, Phys. Rev. Lett. **128**, 047001 (2022).

[18] J. Bi, Y. Nakamoto, P. Zhang, K. Shimizu, B. Zou, H. Liu, M. Zhou, G. Liu, H. Wang, and Y. Ma, Giant enhancement of superconducting critical temperature in substitutional alloy $(La, Ce)H_9$, Nat. Commun. **13**, 5952 (2022).

[19] W. Chen, X. Huang, D. V. Semenok, S. Chen, D. Zhou, K. Zhang, A. R. Oganov, and T. Cui, Enhancement of superconducting properties in the La–Ce–H system at moderate pressures, Nat. Commun. **14**, 2660 (2023).

[20] G. Huang, D. Peng, T. Luo, L.-C. Chen, P. Dalladay-Simpson, Z.-Y. Cao, F. A. Gorelli, G.-H. Zhong, H.-Q. Lin, and X.-J. Chen, Synthesis of superconducting phase of $La_{0.5}Ce_{0.5}H_{10}$ at high pressures, J. Phys.: Condens. Matter **36**, 075702 (2024).

[21] S. Di Cataldo and L. Boeri, Metal borohydrides as ambient-pressure high-T_c superconductors, Phys. Rev. B **107**, L060501 (2023).

[22] D. V. Semenok, A. G. Kvashnin, A. G. Ivanova, V. Svitlyk, V. Y. Fominski, A. V. Sadakov, O. A. Sobolevskiy, V. M. Pudalov, I. A. Troyan, and A. R. Oganov, Superconductivity at 161 K in thorium hydride ThH_{10}: Synthesis and properties, Mater. Today **33**, 36 (2020).

[23] X. Li, X. Huang, D. Duan, C. J. Pickard, D. Zhou, H. Xie, Q. Zhuang, Y. Huang, Q. Zhou, B. Liu *et al.*, Polyhydride CeH_9 with an atomic-like hydrogen clathrate structure, Nat. Commun. **10**, 3461 (2019).

[24] N. P. Salke, M. M. Davari Esfahani, Y. Zhang, I. A. Kruglov, J. Zhou, Y. Wang, E. Greenberg, V. B. Prakapenka, J. Liu, A. R. Oganov *et al.*, Synthesis of clathrate cerium superhydride CeH_9 at 80–100 GPa with atomic hydrogen sublattice, Nat. Commun. **10**, 4453 (2019).

[25] W. Chen, D. V. Semenok, X. Huang, H. Shu, X. Li, D. Duan, T. Cui, and A. R. Oganov, High-temperature superconducting phases in cerium superhydride with a T_c up to 115 K below a pressure of 1 megabar, Phys. Rev. Lett. **127**, 117001 (2021).

[26] I. A. Kruglov, A. G. Kvashnin, A. F. Goncharov, A. R. Oganov, S. S. Lobanov, N. Holtgrewe, S. Jiang, V. B. Prakapenka, E. Greenberg, and A. V. Yanilkin, Uranium polyhydrides at moderate pressures: Prediction, synthesis, and expected superconductivity, Sci. Adv. **4**, eaat9776 (2018).

[27] D. Zhou, D. V. Semenok, D. Duan, H. Xie, W. Chen, X. Huang, X. Li, B. Liu, A. R. Oganov, and T. Cui, Superconducting praseodymium superhydrides, Sci. Adv. **6**, eaax6849 (2020).

[28] D. Zhou, D. V. Semenok, H. Xie, X. Huang, D. Duan, A. Aperis, P. M. Oppeneer, M. Galasso, A. I. Kartsev, A. G. Kvashnin *et al.*, High-pressure synthesis of magnetic neodymium polyhydrides, J. Am. Chem. Soc. **142**, 2803 (2020).

[29] N. N. Wang, P. F. Shan, K. Y. Chen, J. P. Sun, P. T. Yang, X. L. Ma, B. S. Wang, X. H. Yu, S. Zhang, G. F. Chen *et al.*, A low-T_c superconducting modification of Th_4H_{15} synthesized under high pressure, Supercond. Sci. Technol. **34**, 034006 (2021).

[30] See Supplemental Material at http://link.aps.org/supplemental/10.1103/PhysRevB.110.024513 for more details about methods, phonon band structure, the ternary convex hull, the

crystalline orbital Hamiltonian population, the COBI, charge transfers, and electronic structure, and which includes Refs. [31–45].

[31] K. Xia, H. Gao, C. Liu, J. Yuan, J. Sun, H.-T. Wang, and D. Xing, A novel superhard tungsten nitride predicted by machine-learning accelerated crystal structure search, Sci. Bull. **63**, 817 (2018).

[32] J. Wang, H. Gao, Y. Han, C. Ding, S. Pan, Y. Wang, Q. Jia, H.-T. Wang, D. Xing, and J. Sun, MAGUS: Machine learning and graph theory assisted universal structure searcher, Natl. Sci. Rev. **10**, nwad128 (2023).

[33] G. Kresse and J. Furthmüller, Efficient iterative schemes for *ab initio* total-energy calculations using a plane-wave basis set, Phys. Rev. B **54**, 11169 (1996).

[34] P. E. Blöchl, Projector augmented-wave method, Phys. Rev. B **50**, 17953 (1994).

[35] P. Giannozzi, S. Baroni, N. Bonini, M. Calandra, R. Car, C. Cavazzoni, D. Ceresoli, G. L. Chiarotti, M. Cococcioni, I. Dabo *et al.*, QUANTUM ESPRESSO: A modular and open-source software project for quantum simulations of materials, J. Phys.: Condens. Matter **21**, 395502 (2009).

[36] C. Liu, H. Gao, Y. Wang, R. J. Needs, C. J. Pickard, J. Sun, H.-T. Wang, and D. Xing, Multiple superionic states in helium–water compounds, Nat. Phys. **15**, 1065 (2019).

[37] Q. Gu, D. Xing, and J. Sun, Superconducting single-layer T-graphene and novel synthesis routes, Chin. Phys. Lett. **36**, 097401 (2019).

[38] C. Liu, J. Shi, H. Gao, J. Wang, Y. Han, X. Lu, H.-T. Wang, D. Xing, and J. Sun, Mixed coordination silica at megabar pressure, Phys. Rev. Lett. **126**, 035701 (2021).

[39] J. P. Perdew, K. Burke, and M. Ernzerhof, Generalized gradient approximation made simple, Phys. Rev. Lett. **77**, 3865 (1996).

[40] A. Togo and I. Tanaka, First principles phonon calculations in materials science, Scr. Mater. **108**, 1 (2015).

[41] R. Dronskowski and P. E. Bloechl, Crystal orbital Hamilton populations (COHP): Energy-resolved visualization of chemical bonding in solids based on density-functional calculations, J. Phys. Chem. **97**, 8617 (1993).

[42] P. C. Müller, C. Ertural, J. Hempelmann, and R. Dronskowski, Crystal orbital bond index: Covalent bond orders in solids, J. Phys. Chem. C **125**, 7959 (2021).

[43] R. Nelson, C. Ertural, J. George, V. L. Deringer, G. Hautier, and R. Dronskowski, LOBSTER: Local orbital projections, atomic charges, and chemical-bonding analysis from projector-augmented-wave-based density-functional theory, J. Comput. Chem. **41**, 1931 (2020).

[44] W. L. McMillan, Transition temperature of strong-coupled superconductors, Phys. Rev. **167**, 331 (1968).

[45] P. B. Allen and R. C. Dynes, Transition temperature of strong-coupled superconductors reanalyzed, Phys. Rev. B **12**, 905 (1975).

[46] H. Olijnyk, S. K. Sikka, and W. B. Holzapfel, Structural phase transitions in Si and Ge under pressures up to 50 GPa, Phys. Lett. A **103**, 137 (1984).

[47] S. J. Duclos, Y. K. Vohra, and A. L. Ruoff, hcp to fcc transition in silicon at 78 GPa and studies to 100 GPa, Phys. Rev. Lett. **58**, 775 (1987).

[48] C. J. Pickard and R. J. Needs, Structure of phase III of solid hydrogen, Nat. Phys. **3**, 473 (2007).

[49] M. Martinez-Canales, A. R. Oganov, Y. Ma, Y. Yan, A. O. Lyakhov, and A. Bergara, Novel structures and superconductivity of silane under pressure, Phys. Rev. Lett. **102**, 087005 (2009).

[50] W. Cui, J. Shi, H. Liu, Y. Yao, H. Wang, T. Iitaka, and Y. Ma, Hydrogen segregation and its roles in structural stability and metallization: Silane under pressure, Sci. Rep. **5**, 13039 (2015).

[51] Y. Li, G. Gao, Y. Xie, Y. Ma, T. Cui, and G. Zou, Superconductivity at ∼100 K in dense $SiH_4(H_2)_2$ predicted by first principles, Proc. Natl. Acad. Sci. USA **107**, 15708 (2010).

[52] A. G. Kvashnin, D. V. Semenok, I. A. Kruglov, I. A. Wrona, and A. R. Oganov, High-temperature superconductivity in a Th–H system under pressure conditions, ACS Appl. Mater. Interfaces **10**, 43809 (2018).

[53] Y. Sun, J. Lv, Y. Xie, H. Liu, and Y. Ma, Route to a superconducting phase above room temperature in electron-doped hydride compounds under high pressure, Phys. Rev. Lett. **123**, 097001 (2019).

[54] B. Lilia, R. Hennig, P. Hirschfeld, G. Profeta, A. Sanna, E. Zurek, W. E. Pickett, M. Amsler, R. Dias, M. I. Eremets *et al.*, The 2021 room-temperature superconductivity roadmap, J. Phys.: Condens. Matter **34**, 183002 (2022).

[55] W. Sun, C. J. Bartel, E. Arca, S. R. Bauers, B. Matthews, B. Orvañanos, B.-R. Chen, M. F. Toney, L. T. Schelhas, W. Tumas *et al.*, A map of the inorganic ternary metal nitrides, Nat. Mater. **18**, 732 (2019).

[56] J. Lim, A. C. Hire, Y. Quan, J. S. Kim, S. R. Xie, S. Sinha, R. S. Kumar, D. Popov, C. Park, R. J. Hemley *et al.*, Creating superconductivity in WB_2 through pressure-induced metastable planar defects, Nat. Commun. **13**, 7901 (2022).

[57] R. G. Parr and R. G. Pearson, Absolute hardness: Companion parameter to absolute electronegativity, J. Am. Chem. Soc. **105**, 7512 (1983).

[58] X. Dong, A. R. Oganov, H. Cui, X.-F. Zhou, and H.-T. Wang, Electronegativity and chemical hardness of elements under pressure, Proc. Natl. Acad. Sci. USA **119**, e2117416119 (2022).

[59] R. G. Pearson, Chemical hardness and the electronic chemical potential, Inorg. Chim. Acta **198**, 781 (1992).

[60] I. Errea, M. Calandra, C. J. Pickard, J. R. Nelson, R. J. Needs, Y. Li, H. Liu, Y. Zhang, Y. Ma, and F. Mauri, Quantum hydrogen-bond symmetrization in the superconducting hydrogen sulfide system, Nature (London) **532**, 81 (2016).

[61] I. Errea, F. Belli, L. Monacelli, A. Sanna, T. Koretsune, T. Tadano, R. Bianco, M. Calandra, R. Arita, F. Mauri *et al.*, Quantum crystal structure in the 250-kelvin superconducting lanthanum hydride, Nature (London) **578**, 66 (2020).

[62] L. Monacelli, I. Errea, M. Calandra, and F. Mauri, Pressure and stress tensor of complex anharmonic crystals within the stochastic self-consistent harmonic approximation, Phys. Rev. B **98**, 024106 (2018).

[63] C. J. Pickard, I. Errea, and M. I. Eremets, Superconducting hydrides under pressure, Annu. Rev. Condens. Matter Phys. **11**, 57 (2020).